PROCEEDINGS OF SPIE

SPIEDigitalLibrary.org/conference-proceedings-of-spie

Holographic solar concentrators stored in an eco-friendly photopolymer

Marta Morales-Vidal, Manuel Ramírez, Kheloud Berramdane, Tomás Lloret, Sergi Gallego, et al.

Marta Morales-Vidal, Manuel G. Ramírez, Kheloud Berramdane, Tomás Lloret, Sergi Gallego, Augusto Beléndez, Inmaculada Pascual, "Holographic solar concentrators stored in an eco-friendly photopolymer," Proc. SPIE 11774, Holography: Advances and Modern Trends VII, 117740V (18 April 2021); doi: 10.1117/12.2592302

SPIE.

Event: SPIE Optics + Optoelectronics, 2021, Online Only

Holographic Solar Concentrators stored in an Eco-friendly Photopolymer

Marta Morales-Vidal*[a], Manuel G. Ramírez[a], Kheloud Berramdane[a], Tomás LLoret[b], Sergi Gallego[c], Augusto Beléndez[c], Inmaculada Pascual[b]
[a]Universidad de Alicante, I.U. Física Aplicada a las Ciencias y las Tecnologías, POB 99, E-03080 Alicante, (SPAIN); [b]Universidad de Alicante, Dept. de Óptica Farmacología y Anatomía, POB 99, E-03080 Alicante, (SPAIN); [c]Universidad de Alicante, Dept. Física Ingeniería de Sistemas y Teoría de la Señal, POB 99, E-03080 Alicante, (SPAIN)

ABSTRACT

In this work it is shown the first characterization of holographic solar concentrators recorded in Biophotopol - one of the greenest photopolymers. Biophotopol is an acrylate-based and water-soluble photopolymer with good recycling properties. The composition of this photopolymer and their thickness are easily changeable, which implies an important advantage vs. others commercialized photopolymers. Good diffraction efficiency and wide acceptance angles are achieved on phase volume transmission holograms by using an optimized composition and thin layers. A curing stage with a white incoherent light has been performed to obtain high temporal stability together with a good diffraction efficiency. Finally, the performance of the holographic lenses as holographic solar concentrators has been evaluated with an electronic setup connected to a polycrystalline silicon photovoltaic cell and a high intensity solar simulator emitting a standard solar spectrum (AM1.5G).

Keywords: Holography, holographic recording materials, photopolymers, low-toxicity photopolymer, solar concentrators

1. INTRODUCTION

The production of energy in a clean and efficient way is a challenge that has a great impact both ecologically and economically on our society. In this sense, it is possible to convert sunlight into energy through thermal energy production systems and photovoltaic energy systems. Thermal energy production systems require very high levels of solar radiation independent of the spectral wavelength. But to achieve high levels of solar radiation is not that important on photovoltaic energy production systems, in this case the energy of the incident photons is determinant. Photons with energy lower than the semiconductor bandgap value will not be absorbed, causing transmission losses or thermalization losses to the photocell. More energetic photons will deliver part of the energy to the PV cell, and the rest will be also thermalized. Some of the semiconductor materials used in photovoltaic cells are summarized below, ordered according to their cut-off wavelength value: $InGaP_2$ (670 nm), GaAs (870 nm), Si (1100 nm), InGaAs (1653 nm), GaSb (1750 nm). In general, efficient photovoltaic cells have high production cost, which is why optical concentrating elements are frequently used to reduce the needed surface of the photocell. As photovoltaic cells are spectrally selective systems with different spectral response curves, the use of volume holographic lenses[1] with chromatic selectivity seems a very promising solution. Point holograms allows to concentrate each part of the sunlight spectrum at different points, well at different photocells (positioned in such a way as to be exposed to that part of the spectrum at which they are most efficient) or even outside the photovoltaic cell. Taking also into consideration the relative movement of the sun[2] with respect to the solar cell and with respect to the solar concentrator, the angular selectivity of the holographic element used has been an important issue to evaluate. Different research groups have developed holographic solar concentrators based on commercial photopolymers as Bayfol HX[3,4], dichromated gelatine[5,6] or different compositions based on acrylamide[7]. Nowadays, only the company PRISM SOLAR modules has managed to present some holographic concentrators based on dichromate gelatine, whereas, this technology is not yet advanced enough to be able to expand in the market. There are some publications about HLs recorded in Biophotopol material[8,9], but this is the first time that it is presented an experimental characterization of the HLs recorded in this low-toxicity material for solar applications. The output current measurements of the PV cell as a function of the incidence angle to the HLs were carried with a solar simulator (standard solar spectrum AM1.5G).

Holography: Advances and Modern Trends VII, edited by Antonio Fimia, Miroslav Hrabovský, John T. Sheridan, Proc. of SPIE Vol. 11774, 117740V · © 2021 SPIE
CCC code: 0277-786X/21/$21 · doi: 10.1117/12.2592302

2. METHODS

2.1 Photopolymer preparation

The material used to record volume phase transmission HLs was an environmentally friendly photopolymer, called Biophotopol[10,11]. The prepolymer solution in water was prepared in our laboratory, under red light conditions, with the following water soluble components: poly(vinyl alcohol) (PVA) as inert binder polymer (Mw = 130000 g/mol, hydrolysis grade = 87.7 %), sodium acrylate solution (polymerizable monomer) as 1:1 acid-base reaction of acrylic acid with sodium hydroxide (NaOH), 5'-riboflavin monophosphate (RF) as sensitizer dye, triethanolamine (TEA) as plasticizer and co-initiator of the photoreaction on the photopolymer layer. The concentration of each component in the prepolymer solution was: 13.0 w/w%, 0.39 M, 1.0×10^{-3} M, 9.0×10^{-3} M for PVA, NaAO, RF, and TEA, respectively. The prepolymer solution was manually deposited over each levelled squared glass substrates of size (6.5×6.5) cm^2 and thickness h_{glass} = 210 µm; after that, the samples were stored inside an incubator under controlled conditions of humidity (60 %) and temperature (20°C). The photopolymer layers were ready for recording when part of the water is evaporated and equilibrium with the environmental conditions inside the incubator was achieved. Then, the HLs recorded were placed under a white LED lamp (13.5W, 875 lm at 6500 K, 30° Lexman) for 5 minutes and at 37.5 cm of distance between the lamp and the sample. The described incoherent light photocuring stage was carried out to ensure high temporal stability and good diffraction efficiency. The physical thickness of the holographic lenses was measured with a micrometer screw (sensitivity of ± 0.001 mm) at the end of the experiment.

2.2 Setup for recording and reading-out holographic lens

Symmetric holographic setup has been used to record unslanted HLs. A diode-pumped laser emitting at 473 nm was spatially filtered and then split into two secondary beams (object and reference) with an intensity ratio 1:1. The collimated reference beam impinge to the photopolymer, while the object beam passed through a refractive lens (RL) and the converging beam focalize at a distance $d_{RL\text{-}PL}/2$ reaching to the photopolymer surface with the same spot size as the reference beam (0.5 cm). The object and reference beams were recombined at the photopolymer with the same object and reference angle $\theta_o = \theta_r = 12.6°$ with respect to normal incidence (Fig. 1). The sum of both intensities recording beam was 1 mW/cm^2, the exposure time was adjusted to obtain the maximum diffraction. The transmitted and diffracted intensity were measured in real time while recording (with a He-Ne laser at with RF is not sensitive). The HLs readout was evaluated at different reconstruction angles by spinning the sample with a rotating platform around its vertical axis.

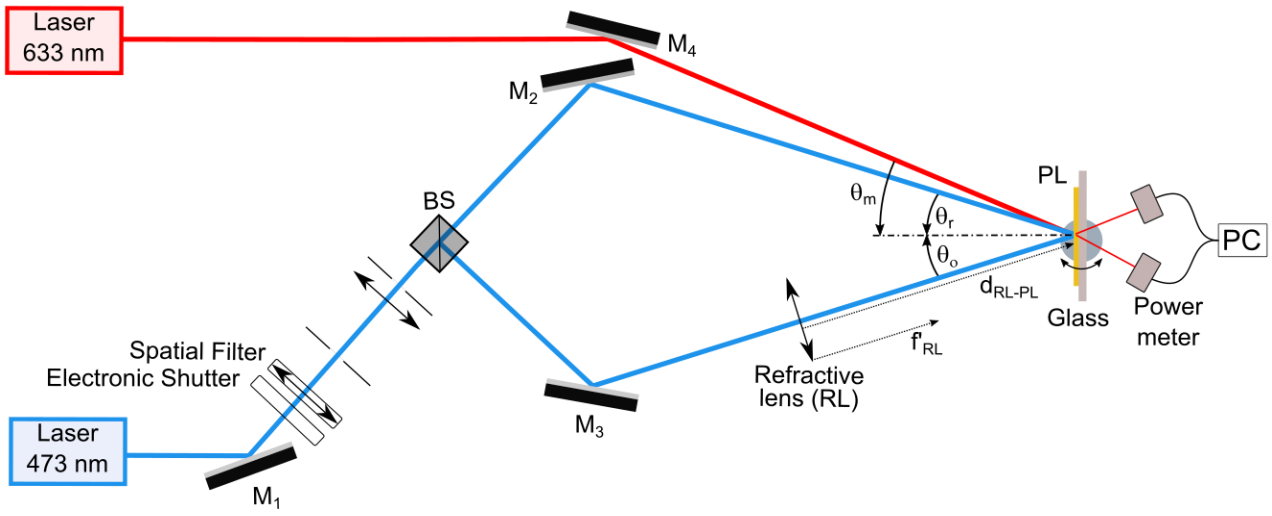

Figure 1. Recording and reconstructing HLs setup. Mi: mirrors; BS: beam splitter; $d_{RL\text{-}PL}$: distance between the refractive lens to the photopolymer; f'_{RL}: focal length of the refractive lens; θ_o and θ_r: object and reference recording angles; θ_m: measuring angle of reconstructing beam; PL: photopolymer layer; PC: computer.

2.3 Solar holographic concentrator setup

The characterization of the HLs as holographic solar concentrators has been performed in a setup illuminated by a solar simulator (model 10500, ABET technologies) which emits a high intensity light output with UV, visible and infrared wavelength, particularly the standard solar spectrum AM1.5G atmospheric. The sun must be considered as a point source with collimated beams and with high spatial uniformity[12]. For this reason, the divergent solar simulator emission was collimated and spatially filtered by using an arrangement of positive lenses and diaphragms. The first diaphragm was placed in the image focal point of the first lens, and at the same time in the object focal point of the second lens. The negative HLs were illuminated by the glass side with the conjugated beam[13] to use them as convergent lens. The HL was illuminated at different reconstructing angles (θ_c) by using a rotating platform (Fig. 2). The polycrystalline silicon PV cell of dimensions (2.5 × 5) cm was placed at its corresponding $f'_{HL\text{-}473}$. The voltage and the current characteristic of the illuminated solar cell were measured by two multimeters connected to a circuit with a variable resistor.

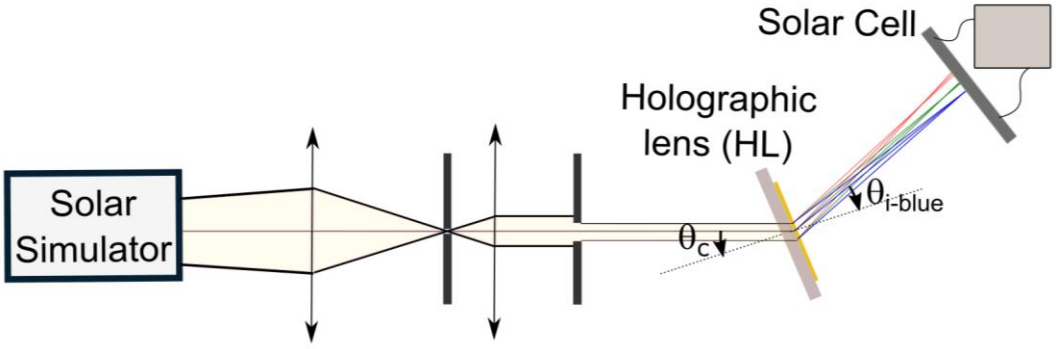

Figure 2.- Holographic solar concentrator setup. θ_c: reconstructing angle, θ_i: image angle of each wavelength.

3. RESULTS

3.1 Geometrical Analysis of the Holographic Lenses

In this work it has been recording four symmetric volume phase holographic lenses by using three different RL: f'_{RL1} = +5 cm, f'_{RL2} = +10 cm, f'_{RL3} = +15 cm placed at a distance $2f'$ from the photopolymer layer. The gaussian focus (f) of the recorded HLs to the first order of diffraction and reconstructing with a plane wave can be obtained as[14]:

$$\frac{1}{f} = \mu\left(\frac{1}{R_o} - \frac{1}{R_R}\right) \quad (1)$$

where μ is the ratio between the reconstructing and the recording wavelength (λc / λr); R_o and R_R is the distance between the object and the reference to the center of the lens, respectively. Although the focal length of the HLs recorded at 473 nm are negative, we use them as positive HLs (HL-1: f'_{HL1} = +5 cm; HL-2: f'_{HL2} = +10 cm; HL-3a and HL-3b: f'_{HL2} = +15 cm) by illuminating them with the conjugated beam on the glass side.

3.2 Optical Analysis of Holographic Lenses

In order to estimate the optical power diffracted in the first diffracted order of the HLs, the diffraction efficiency was studied by using a He-Ne laser. The ratio between the optical power diffracted by the first order and the incident power has been represented as a function of the angular deviation from Bragg angle. The diffraction efficiency was good in all HLs at 633 nm wavelength, around 90%. The angular width of the HLs prepared varies between 1.8-2.7° (obtained between minimums of the DE curve vs angle). The angular width was around 1.9° in HL-1, HL-2, and HL-3b (Fig. 3a). The similar widths shown were due to the very similar photopolymer layer thickness (90 ± 5 μm). A wider width (2.7°) was obtained in HL-3a with a thinner layer thickness. In figure 3b it is compared HL-3a and HL-3b with the same focal length but different thickness 65 and 90 μm, respectively. The small differences between angular widths are related with the small differences on the thickness of the layers, due to the recording angle of all HLs studied was the same, and therefore the central frequency was the same.

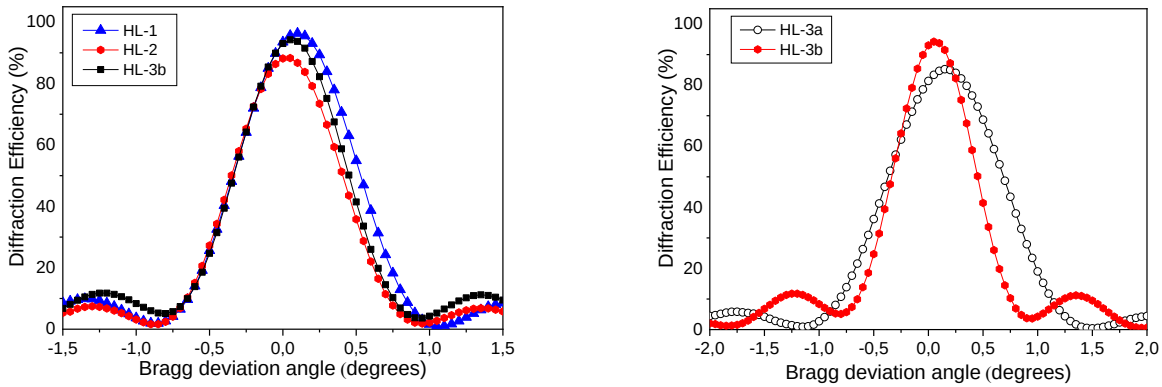

Figure 3.- Diffraction efficiency (DE) at 633 nm from holographic lenses as a function of angular deviation from the Bragg angle.

3.3 Holographic solar concentrators

Solar concentrators usually incorporate two-axis tracking to follow the trajectory of the sun (hourly movement and seasonal movement). Therefore, to make the most of solar radiation, it is important to consider the acceptance angle of holographic solar concentrators. The acceptance angle for the recording HLs depends on the thickness, it was shown that at a single wavelength is between 1.8° - 2.7 °. To evaluate the behavior of HLs acting as solar concentrators (illuminated by several wavelengths), the electrical current produced by a PV cell as a function of the incidence angle between the solar simulator beam and the normal to the HLs was measured. These results have been compared with the ideal angular conditions in a grating of 922 l/mm illuminated by different wavelength (-12.6°, -14.2° and -17.0° at λc = 473, 532 and 633 nm, respectively), and the theoretical reconstructing angles obtained by[14]:

$$\sin(\theta i) = \sin(\theta c) + \mu\,[\sin(\theta o) - \sin(\theta r)] \qquad (2)$$

where θ is the off-axis angle in general, and i, c, o, r are the indices of the image, reconstruction, object, and reference waves, respectively. The image angle calculated for the following wavelength (λc = 473, 532, 633 nm) at the incidence angle θc = θo = θr = -12.6°, are θi = 12.6°, θi = 15.8°, and 21.5°.

In Figure 4, a sharp current increase is observed at 10°, when blue radiation begins to illuminate the PV cell. This current was maximum around 12.6°, when the incidence angle match with the Bragg angle to the recording wavelength (473 nm). And a high current was maintained for the three HLs studied until around 17°, the ideal angular conditions in red light (633 nm). For a current intensity of 80% or higher, the experimental angular width obtained from figure 4 is about 12°. Therefore, the theoretically calculated values are in concordance with the experimental results, the current intensity remains constant since the PV cell start to be illuminated with blue until the red emission stops to impinge to the photocell when HLs with long focal length are used. In the case of LH_1 (f'_{LH} = 5 cm) it was shown a high output current even on angles of incidence higher than 24°. This high output current during a wider angle it can be explained because the second order of diffraction also impinge to the PV cell, because it was closer than the HL-2 and HL-3 and this allows to collect a broader interval of wavelength even at very high incidence angle.

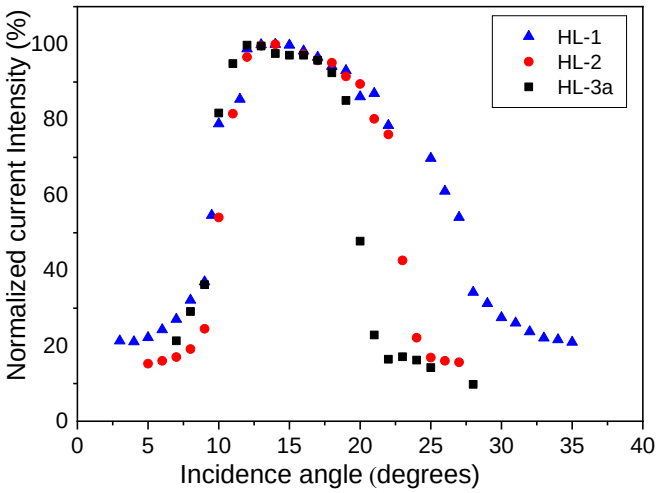

Figure 4.- Normalized current intensity as a function of the angle of incidence (between the solar simulator beam to the normal of the photopolymer). The output current was measured as a function of the rotation angle of the HL respect to its vertical axis.

4. CONCLUSIONS

As a conclusion of this work, we can remark that the diffraction efficiency achieved for HLs is around 90% at reconstruction wavelength of 633 nm. At the same time, the angular width by using the same wavelength is 2.7°. We can improve the angular width by using white light from a solar simulator, in this case 9° for maximum current. For current of 80% of higher the angular width reaches 12°. First characterization of HLs recorded in Biophotopol as solar concentrators has been performed.

ACKNOWLEDGMENTS

This work has financial support from: Ministerio de Ciencia e Innovación, Spain, under project PID2019-106601RB-I00 and FIS2017-82919-R/(MINECO/AE/FEDER, UE); Generalitat Valenciana, Spain, under project CDEIGENT/2018/024.

REFERENCES

[1] Schwar, M. J. R., Pandya T. P., & Weinberg, F. J., “Point Holograms as Optical Elements,” Nature, 215, 239-241 (1967).
[2] Vieira da Rosa A., [Fundamentals of Renewable Energy Processes], Elsevier, 495-522 (2013).
[3] Bañares-Palacios, P., Álvarez-Álvarez, S., Marín-Sáez, J., Collados, M.-V., Chemisana, D. & Atencia, J., “Broadband behavior of transmission volume holographic optical elements for solar concentration,” Opt. Express 23(11), A671 (2015).
[4] Kao H., Ma J., Wang C., Wu T., & Su P., “Crosstalk-Reduced Double-Layer Half-Divided Volume Holographic Concentrator for Solar Energy Concentration,” Sensors, (2020).
[5] Ferrara, M. A., Striano, V., & Coppola, G.. “Volume Holographic Optical Elements as Solar Concentrators: An Overview. Applied Sciences,” 9(1), 193, (2019).

[6] Stojanoff, C. G., Schütte, H., Schulat, J., Kubiza, R., & Froning, P. “Fabrication of large format holograms in dichromated gelatin films for sun control and solar concentrators,” *Proc. SPIE 3010*, Diffractive and Holographic Device Technologies and Applications IV, 3010 (1997).
[7] Akbari, H., Naydenova, I., & Martin, S. “Using acrylamide-based photopolymers for fabrication of holographic optical elements in solar energy applications,” Applied Optics, 53(7), 1343-1353 (2014).
[8] Lloret, T., Navarro-Fuster, V., Ramírez, M. G., Ortuño, M., Neipp, C., Beléndez, A. & Pascual, I., “Holographic lenses in an environment-friendly photopolymer,” Polymers 10(302) (2018).
[9] Lloret, T., Navarro-fuster, V., Ramírez, M. G., Morales-Vidal, M., Beléndez, A., & Pascual, I. (2020). “Aberration-Based Quality Metrics in Holographic Lenses,” Polymers 12(4), 993 (2020).
[10] Ortuño, M., Fernández, E., Gallego, S., Beléndez, A. & Pascual, I., “New photopolymer holographic recording material with sustainable design,” Opt. Express 15(19), 12425-12435 (2007).
[11] Ortuño, M.; Gallego, S.; Márquez, A.; Neipp, C.; Pascual, I.; & Beléndez, A. “Biophotopol: A Sustainable Photopolymer for Holographic Data Storage Applications,”. Materials, 5, 772–783 (2012).
[12] Domínguez, C., Antón, I., & Sala, G. “Solar simulator for concentrator photovoltaic systems,”. Optics Express, 16(19) (2008).
[13] Kostuk, R.K. Holography Principles and Applications; CRC Press: Boca Raton, FL, USA, (2019).
[14] Champagne, E. B. “Nonparaxial Imaging, Magnification, and Aberration Properties in Holography”. Journal of the Optical Society of America,” *57*(1), 51(1967).
[15] Morales-Vidal, M., Ramírez, M. G., Sirvent, D., Martínez-Guardiola, F. J., Álvarez, M. L., & Pascual, I. “Efficient and stable holographic gratings stored in an environmentally friendly photopolymer,”. Proceedings of SPIE - The International Society for Optical Engineering, 11207 (2019).